Transmission of stress induced electric signals in dielectric media

P. Varotsos,[a] N. Sarlis, M. Lazaridou, and P. Kapiris
Solid Earth Physics Institute, University of Athens, Panepistimiopolis, Zografos, Athens 157 84, Greece

(Received 16 September 1997; accepted for publication 24 September 1997)

The conditions under which pressure (stress) variations on solids, containing charged defects, can lead to the emission of transient electric signals, are discussed. The resulting electric field E varies as $1/d^3$ (where d denotes the distance from the emitting source), in the simple case when the surrounding medium is homogeneous and isotropic. We show that this behavior changes to $1/d$ when studying the electric field within a cylindrical channel of radius R and infinite length having conductivity appreciably larger than that of the host medium; this holds up to a certain (reduced) distance d/R, which increases versus the conductivity ratio. We also investigate the variation of the electric field, versus the distance, inside a layer of width w and infinite extent having conductivity appreciably larger than that of the host medium; we then find that the electric field decreases as $1/d^2$, in a wide range of distances up to a certain value of d/w, which is controlled by the conductivity ratio. In both conductive paths, i.e., cylinder and layer, the electric field approaches the $1/d^3$ behavior, but only at very large values of d/R and d/w, respectively, reaching the value that would be measured if the host medium was solely present. This implies a high current density inside the path. The case, when the highly conductive path terminates within the host medium, is also discussed; it is found that the ''edge effects'' play a prominent role in electric field values measured within the host medium, but close to the outcrop of the path. It is shown that a simplified calculation could erroneously obtain electric field values that are several orders of magnitude smaller than those calculated in this article. As an example, the transmission of low frequency electric signals in the earth is discussed. It is concluded that charged-defect generation mechanisms lead to electric field values that are measurable at large distances. © *1998 American Institute of Physics.* [S0021-8979(98)03201-0]

I. INTRODUCTION

The variation of the (hydrostatic) pressure (P) affects the formation Gibbs free energy (g^f) as well as the migration Gibbs free energy (g^m) of defects in solids. The defect volumes for the formation process (v^f) and migration process (v^m) are defined as:[1] $v^f=(dg^f/dP)_T$, $v^m=(dg^m/dP)_T$, where T denotes the temperature. In experiments that involve both formation and migration of defects, the results are described in terms of an activation Gibbs free energy g^{act}, which is associated with an activation volume $v^{\mathrm{act}}=(dg^{\mathrm{act}}/dP)_T$. Lazarus and co-workers[2] published a series of pioneering experiments studying the influence of pressure on ionic conductivity and on diffusion coefficients in various materials. In most materials v^{act} was found to be positive, but negative values have been also reported, e.g., in B4-AgI. (A tentative explanation of the latter experimental result was discussed in Ref. 3). Negative v^{act} has been also found in water, as well as in some polymers (containing water), in which the electrical conductivity—in a certain region—is controlled more by the water than by the polymer.[4]

Defects in solids are associated with polarization (or depolarization) effects.[5–7] In ionic crystals, point defects may carry an effective electric charge (e.g., in NaCl the crystal contains Schottky defects: cation vacancies with effective charge $-e$ and anion vacancies with effective charge $+e$; on the other hand, in AgCl and AgBr, the native thermally produced defect is the cation Frenkel defect: interstitial silver ions with effective charge $+e$ are compensated by cation vacancies). In the deep interior of a pure and otherwise perfect crystal, the two components of the appropriate defect pair have equal concentrations and the net charge density is zero. This, however, does not hold near any atomic configurations which can act as a source and sink for the individual components of the defect pair[6] (e.g., the jogs on edge dislocations and kinks on the steps of surfaces—each have an exposed and partially uncompensated ion, with an effective charge of $\pm e/2$—act as point defect sources and sinks). This leads, at steady state, to an ionic surface charge, compensated by a space charge of opposite sign, which reflects strong electric field values reaching 10^6 V/cm near the surface[6] and plays an important role in the mass transport in ionic crystals. Similar electrical charge effects occur on dislocations; this line of charge is compensated by a cylindrically symmetric space charge, centered along the dislocation, and consisting of point defects—e.g., vacancies and heterovalent impurity ions—with an effective charge of sign opposite of that on the dislocation core.[6] Aliovalent impurities play an important role in the ''extrinsic'' (low temperature) range. For example, the presence of M^{2+} impurities in a crystal A^+B^- introduces an equivalent number of cation vacancies, in order to maintain charge neutrality in the bulk. A portion of these cation vacancies (negative effective charge) are attracted by the divalent cations and form electric dipoles that can change their orientation in space. For simplicity, we may assume that this change of orientation can be achieved only through jumps of the neighboring cations into

[a]Electronic mail: pvaro@leon.nrcps.ariadne-t.gr

 0021-8979/98/83(1)/60/11/$15.00

the cation vacancies, which are usually called ''bound'' cation vacancies; this bound (b) cation vacancy motion requires a migration Gibbs free energy $g^{m,b}$, which corresponds to a migration volume $v^{m,b}=(dg^{m,b}/dP)_T$. The (re)orientation of these dipoles greatly affects the (low frequency) dielectric constant and leads to the emission of transient (de)polarization currents.[1] Furthermore, the presence of M^{+2} could greatly change the surface charge and/or the measured charge of dislocations.[6]

A pressure (stress) change of an ionic solid induces a time variation of the aforementioned polarization, thus leading to an emission of a transient electric signal (this is discussed in Sec. II). When this emitting solid is surrounded by a medium of conductivity σ', the question arises whether the signal can be observed at large distances, i.e., at distances several times larger than the dimensions of the emitting source. Of special interest, for practical applications, is the case when the emitting source lies at a small distance from a ''path'' of unknown geometry, which has a conductivity σ orders of magnitude larger than the conductivity σ' of the surrounding medium. The study of this case is the main goal of the present article. We first simplify the real situation, assuming that an emitting dipole lies inside the conductive ''path,'' and we solve two boundary value problems:

(a) a cylindrical channel of radius R and infinite length, lying inside a more resistive medium (Sec. III), and
(b) a conductive layer—of infinite extent but with a certain width w—embedded in a more resistive medium (Sec. IV).

The decrease of the electric field is studied at various (reduced) distances d/R and d/w, respectively, for various conductivity ratios σ/σ'. The study is then extended (Sec. V) to the more realistic case when the emitting dipole lies *outside* the conductive path. In Sec. VI, we discuss the consequences of the high conductivity path terminating within the host medium σ'; we conclude that for large conductivity ratios, the ''edge effects'' play a major role, thus leading to high values of the electric field, when it is measured in the host medium but close to the outcrop of the conductive path.

II. PRESSURE (STRESS) STIMULATED CURRENTS (VOLTAGES)

A solid containing electric dipoles, due to defects, can emit ''pressure stimulated currents'' (PSCs), under isothermal conditions, as a result of either increasing or decreasing pressure.[1] They can be classified into two categories: ''pressure stimulated polarization currents'' (PSPCs), or ''pressure stimulated depolarisation currents'' (PSDC). PSPC refers to the polarization that arises, under a *gradual* variation of pressure (pressure increase, if the migration volume $v^{m,b}$ is negative, or pressure decrease, if $v^{m,b}>0$); when the relaxation time (τ) becomes sufficiently small, the electric dipoles align from an initially random orientation into the direction of the continuously acting external or internal electric field. In the PSDC category, the solid is initially brought into a fully polarized state, under the action of an external field for a time appreciably larger than the relaxation time; if $v^{m,b}>0$, the pressure is increased to a final value P_f, thus increasing τ so that the dipoles are practically immobilized and the electric field is then switched off; the pressure is then gradually decreased and a depolarization current density j is liberated, the absolute value of which reaches a maximum j_M at a certain pressure P_M. If $v^{m,b}<0$ the depolarization currents are emitted upon increasing pressure.

A general condition for the appearance of the maximum in the absolute value of the current density j can be derived as follows:

Assuming the operation of a single relaxation time, the current density j is given by

$$j=-\frac{d\Pi}{dt}=\frac{\Pi(t)-\Pi_E}{\tau(t)}$$

where $\Pi(t)$ is the polarization each time, and Π_E the isothermal saturation of polarization (cf. $\Pi_E=0$ for PSDC, Ref. 7). This relation can be also written as: $j\tau(t)=\Pi(t)-\Pi_E$ which by differentiating with respect to time for $T=$constant gives

$$j\frac{d\tau}{dt}+\tau\frac{dj}{dt}=-\frac{d[\Pi(t)-\Pi_E]}{dt}.$$

For free-rotating dipoles, according to Langevin theory, we may write $\Pi_E=\mu^2 N_D E_{\rm loc}/3kT$, where μ is the dipole moment, N_D is the dipole concentration, and $E_{\rm loc}$ the local electric field. In materials for which $E_{\rm loc}$ varies only slightly with pressure,[8] (and if μ, N_D are assumed independent of P) the quantity $d\Pi_E/dt$ can be disregarded, at least in the pressure region when $-d\Pi(t)/dt$ starts to become significant, and hence the previous relation turns to:

$$j\frac{d\tau}{dt}+\tau\frac{dj}{dt}=-j.$$

The maximum value j_M occurs when $dj/dt|_{j=j_M=0,}$ and hence we find

$$\left.\frac{d\tau}{dt}\right|_{j=j_M}=-1.$$

This is the condition for the appearance of a maximum in the absolute value of PSC. It is exact for PSDC (because, in the above derivation, $\Pi_E=0$),[7] but also holds for PSPC as long as the pressure variation of Π_E is insignificant.

The above relation, for any form of the pressure rate

$$b\equiv\left.\frac{dP}{dt}\right|_T,$$

can be alternatively written as:

$$\left.\frac{dP}{dt}\right|_T\left.\frac{d\tau}{dP}\right|_{j=j_M}=-1 \quad \text{or} \quad b\left.\frac{d\tau}{dP}\right|_{j=j_M}=-1$$

which, after considering that[1,7]

$$\left.\frac{\partial\tau}{\partial P}\right|_T=\frac{v^{m,b}}{kT}$$

becomes:

$$\frac{b\upsilon^{m,b}}{kT} = -\frac{1}{\tau(P_M)},$$

where $\tau(P_M)$ denotes the relaxation time at the pressure at which j_M is detected. This relation holds either for PSPC or PSDC, without assuming that the pressure rate b is constant.

Thus, in a previously polarized solid, which contains electric dipoles due to defects, a transient depolarization electric signal is emitted in the absence of any external electric field. It maximizes when a *gradual* pressure variation decreases the relaxation time with a rate obeying the relation $b\upsilon^{m,b}\tau = -kT$. Similarly, if the solid is not initially polarized, a transient polarization electric signal is emitted, under the action of an (external or internal) electric field, which maximizes when $b\upsilon^{m,b}\tau = -kT$.

Slifkin[9] suggested the following mechanism for the production of electric dipoles upon *abrupt* stress variation in materials with significant concentrations of impurities. Such is the case of geophysically interesting materials (as silicates, oxides, and the like) because lattice vacancies and aliovalent impurity ions carry effective charges. The space charge around an electrically charged edge dislocation consists largely of aliovalent ions. These ions will,in general, be substantially less mobile than dislocation segments bowed out between pinning points. Hence, at an *abrupt* change in stress, the bowed dislocation loops will quickly respond (cf. the dislocation loops between the pinning points respond to applied shear stresses much as if they were non-Hookean elastic bands), leaving the space charge distribution unrelaxed; the center of the space charge no longer coincides with the line of the dislocation, and hence an electric dipole is produced. The stress-induced dipole moment lies in the slip plane and is oriented perpendicular to the dislocation line. Slifkin[9] then proceeded to a numerical estimate of the (total) electric dipole moment for a horizontal block 100 m thick and 1000 m wide on the other two sides, that has been folded about a horizontal axis perpendicular to one of the end faces. Assuming that the angle through which the block has been bent is 1° and that the density of the excess dislocations (i.e., new edge dislocations, all of the same mechanical sign, in order to achieve the aforementioned bending) is around $4\times10^7/\mathrm{m}^2$, which probably greatly underestimates[9] the dislocation densities in naturally occurring rocks, Slifkin found a dipole moment of around 8×10^{-4} C m, after first estimating that the stress-induced dipole moment per unit length of dislocation is 2×10^{-19} C m/m; in other words, Slifkin based his estimation on the relation: (stress induced dipole moment of a block) = (stress induced dipole moment per unit length of dislocation) × (density of the excess dislocations) × (cross-sectional area) × (length of the dipole)

In this example Slifkin[9] found an electric field value E of 7×10^{-6} V/m at a distance of 10 km from the dipole by assuming a $1/d^3$ decrease. In the following sections, we consider the transmission of these signals over large distances. A probable mechanism for such a transmission was recently suggested by Lazarus.[10]

III. CONDUCTIVE CYLINDER INSIDE A MEDIUM WITH SMALLER CONDUCTIVITY

A. Point source of current at the center of a cylinder

Let us suppose that the point current (monopole) source I is located at the origin (0,0,0) of a cylindrical system (ρ,φ,z) of coordinates. Further, consider a conductive cylinder, of conductivity σ, with radius R and its axis along the z axis, that lies in the region $\rho<R$. The remaining space is a medium with smaller conductivity σ', i.e., $\sigma'<\sigma$. The electrostatic potential φ is composed of two parts: the primary part φ^p, that is the (singular at the origin) potential of a point current source inside a full space of conductivity σ, and a secondary part φ^s, that is due to the existence of the cylinder. The primary potential has to solve the Poisson's equation $\nabla^2\varphi^p = I/\sigma\ \delta(\mathbf{r})$, so it has the form $\varphi^p = I/[4\pi\sigma(\rho^2+z^2)^{1/2}]$, and can be written as

$$\varphi^p = I/(2\pi^2\sigma R)\int_0^\infty K_0(\xi\rho/R)\cos(\xi z/R)\,d\xi,$$

since[11] $\int_0^\infty K_0(\lambda\rho)\cos(\lambda z)\,d\lambda = \pi/[2(\rho^2+z^2)^{1/2}]$.

Inside (IN) the cylinder the solution involves the singular part φ^p, that describes the point current source, and the secondary part φ^s expressed in terms of the well-behaving at the origin modified Bessel function of the first kind[12] $I_0(\xi\rho/R)$

$$\varphi_{\mathrm{IN}} = \varphi^p + \varphi^s = I/(2\pi^2\sigma R) \times \int_0^\infty [K_0(\xi\rho/R) + A(\xi)I_0(\xi\rho/R)]\cos(\xi z/R)\,d\xi. \quad (1)$$

Outside (OUT) the cylinder, the potential involves only the well-behaving at infinity modified Bessel function of the second kind $K_0(\xi\rho/R)$:

$$\varphi_{\mathrm{OUT}} = I/(2\pi^2\sigma R)\int_0^\infty B(\xi)K_0(\xi\rho/R)\cos(\xi z/R)\,d\xi. \quad (2)$$

The unknown functions $A(\xi)$ and $B(\xi)$ are to be determined from the boundary conditions for the electric field $\mathbf{E} = -\mathrm{grad}\ \varphi$ on the surface of the cylinder $\rho = R$:

$$E_{z\mathrm{IN}}(z,R) = E_{z\mathrm{OUT}}(z,R), \quad (3)$$

$$\sigma E_{\rho\mathrm{IN}}(z,R) = \sigma' E_{\rho\mathrm{OUT}}(z,R). \quad (4)$$

Equation (3) implies

$$K_0(\xi) + A(\xi)I_0(\xi) = B(\xi)K_0(\xi) \quad (5)$$

and Eq. (4), since $K_0'(x) = -K_1(x)$ and $I_0'(x) = I_1(x)$, leads to:

$$\sigma K_1(\xi) - \sigma A(\xi)I_1(\xi) = \sigma' B(\xi)K_1(\xi). \quad (6)$$

A combination of Eqs. (5) and (6) gives:

$$A(\xi) = (\sigma-\sigma')K_1(\xi)K_0(\xi)/[\sigma I_1(\xi)K_0(\xi) + \sigma' I_0(\xi)K_1(\xi)] \quad (7)$$

and

$$B(\xi) = 1 + A(\xi)I_0(\xi)/K_0(\xi). \quad (8)$$

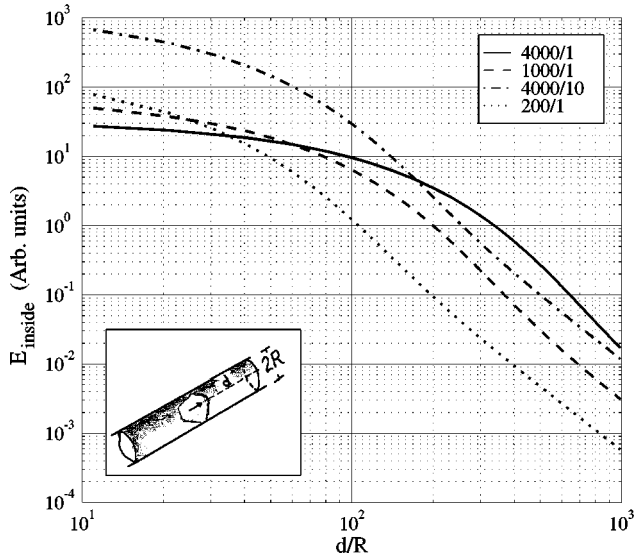

FIG. 1. The electric field E_{inside} vs the (reduced) distance d/R generated by a current dipole lying inside a conductive cylinder (of radius R and conductivity σ) of infinite length embedded in a medium (host) with conductivity σ' ($\sigma > \sigma'$). The curves correspond to the same dipole moment of the emitting source and to the conductivity ratios: $\sigma/\sigma' = 4000/1$, 1000/1, 4000/10, and 200/1, respectively.

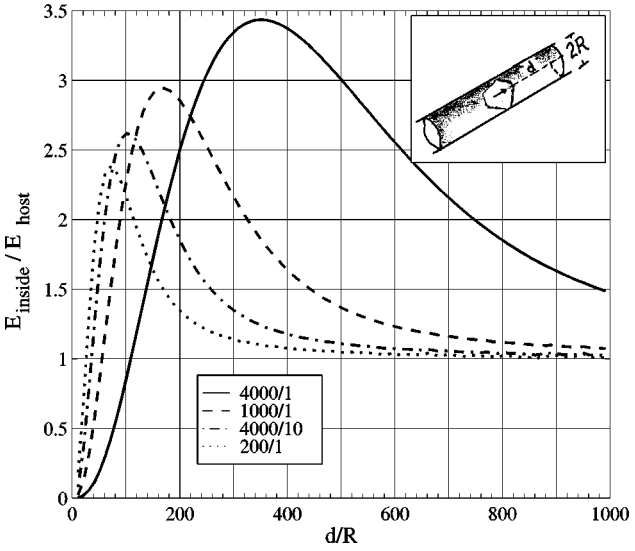

FIG. 2. The ratio $E_{\text{inside}}/E_{\text{host}}$ vs the reduced distance d/R from a current dipole lying inside a conductive cylinder (of radius R and conductivity σ) of infinite length embedded in a medium (host) with conductivity σ' ($\sigma > \sigma'$). The curves correspond to the conductivity ratios: $\sigma/\sigma' = 4000/1$, 1000/1, 4000/10, and 200/1, respectively.

By inserting Eqs. (7) and (8) into Eqs. (1) and (2), respectively, we find the electrostatic potential inside and outside the cylinder.

B. Dipole current source

We consider the case of a dipole current source $\mathbf{p}=\mathbf{I}l$, located at the origin. We first recall the general expression:

$$\varphi_{\text{dipole}} = -\mathbf{p}\cdot \text{grad}\ \varphi_{\text{monopole}}/I \tag{9}$$

and then, using the expressions (1) and (2) for the monopole potential, we can obtain the electrostatic potential for any polarization of the dipole.

For a dipole, $|\mathbf{p}|=Il$, along the z axis, and for points inside the cylinder ($\rho < R$), we obtain:

$$\varphi_{\text{IN}}(\rho,z) = Il/(2\pi^2\sigma R^2)\int_0^\infty [K_0(\xi\rho/R) + A(\xi)I_0(\xi\rho/R)]\xi \sin(\xi z/R)d\xi, \tag{10}$$

while, for points outside the cylinder ($\rho > R$), we have:

$$\varphi_{\text{OUT}}(\rho,z) = Il/(2\pi^2\sigma R^2)\int_0^\infty K_0(\xi\rho/R) \times [1 + A(\xi)I_0(\xi)/K_0(\xi)]\xi \sin(\xi z/R)d\xi. \tag{11}$$

Figure 1 depicts the electric field E_z along the axis of the cylinder at $\rho = 0$ (labeled E_{inside}) versus the distance $d=z$ from the dipole. The ratio of this field to that for a full space of conductivity σ' (labeled E_{host}) is shown in Fig. 2. For a given conductivity ratio, the ratio $E_{\text{inside}}/E_{\text{host}}$ reaches a maximum value, larger than unity, at a certain (critical) reduced distance—defined as $(d/R)_{\text{crit}}$—and then decreases approaching unity at appreciably larger distances. If we recall that E_{host} varies with distance as $1/d^3$, we can conclude that when studying (reduced) distances *smaller* than $(d/R)_{\text{crit}}$, the electric field E_{inside} decreases (versus distance) at a rate slower than $1/d^3$. At distances *appreciably* larger than $(d/R)_{\text{crit}}$, the field E_{inside} varies as $1/d^3$ approaching E_{host}.

The limiting values of the ratio $E_{\text{inside}}/E_{\text{host}}$, as d/R tends to 0 or to infinity, can be easily found using the expression (10). As d/R tends to 0, only the first term of the integral is singular driving $E_{\text{inside}}/E_{\text{host}}$ towards σ'/σ. As d/R tends to infinity, the main contribution of the second term in the integral comes from ξ around 0, where $A(\xi)$ is approximately $(\sigma-\sigma')K_0(\xi)/\sigma'$, so that the ratio $E_{\text{inside}}/E_{\text{host}}$ tends to $(\sigma'/\sigma)[1+(\sigma-\sigma')/\sigma'] = 1$. At intermediate distances, the study of this ratio can be performed as follows: Eq. (10) leads to

$$E_{\text{inside}}/E_{\text{host}} = (\sigma'/\sigma)\left[1 + 2/\pi(d/R)^3 \times \int_0^\infty A(\xi)\xi^2/2\cos(\xi d/R)d\xi\right]. \tag{12}$$

We first investigate the case $\sigma' = 0$, which corresponds to $A(\xi) = K_1(\xi)/I_1(\xi)$. The function $K_1(\xi)\xi^2/[2I_1(\xi)]$, that is to be cosine-transformed according to Eq. (12), tends to 1 as ξ tends to 0, and drops off exponentially to 0 as ξ tends to infinity, thus, it can be considered as composed of two parts: a first part, that is an almost constant function $f_1(\xi)$ of finite support from 0 to ξ_0, and of a second part $f_2(\xi)$, that is an exponentially decreasing tail. The most significant part of the cosine transform,[13] for large values of d/R, comes from $f_1(\xi)$ and is inversely proportional to d/R. Therefore, for $\sigma' = 0$, the ratio $E_{\text{inside}}/E_{\text{host}}$ is proportional to $(d/R)^2$, thus leading to a $1/d$ behavior for the electric field inside the channel.

We now examine the case when σ' is *nonzero*, but $\sigma'/\sigma \ll 1$; we then find that approximately $A(\xi) \approx [K_1(\xi)/I_1(\xi)]\xi I_1(\xi)K_0(\xi)/[\xi I_1(\xi)K_0(\xi)+\sigma'/\sigma]$; the function $\xi I_1(\xi)K_0(\xi)$ is an increasing function of ξ that ranges from 0 to 1/2 at infinity, and hence the function $\Gamma(\xi)=\xi I_1(\xi)K_0(\xi)/[\xi I_1(\xi)K_0(\xi)+\sigma'/\sigma]$, which modulates the previous integral, is an almost constant function that steps from 0 to 1 as ξ passes through ξ_1: $\xi_1 I_1(\xi_1)K_0(\xi_1) = \sigma'/\sigma$. In order to achieve the most significant contribution of this modulation to the previous integral, we can simulate $\Gamma(\xi)$ by the function $\Theta(\xi-\xi_1)$, where $\Theta(x)$ is the Heaviside unit step function; that is $\Theta(x)=0$ if $x<0$, and $\Theta(x) = 1$ if $x>0$. The cosine transform, for large values of d/R, is then mainly dependent on the term: $\sin(\xi_1\, d/R)/(d/R)$ and hence the ratio $E_{\text{inside}}/E_{\text{host}}$ varies as $(d/R)^2 \sin(\xi_1\, d/R)$. Using this dependence of the ratio on d/R to estimate the inflection point $(d/R)_{\text{infl}}$ of the curves in Fig. 1, we find that it is approximately equal to $1.52/\xi_1$; note that $(d/R)_{\text{crit}}$ exceeds $(d/R)_{\text{infl}}$ by a factor of around 2.5.

Summarizing, one can state that, for values smaller than $(d/R)_{\text{infl}}$, the electric field inside the cylinder varies almost as $1/d$. For conductivity ratios $\sigma/\sigma'=4000/1$, 1000/1, 4000/10, and 200/1, used in Fig. 1, the corresponding values of $(d/R)_{\text{infl}}$ are 147, 67, 40, 26, and $(d/R)_{\text{crit}}=351$, 161, 101, and 71, respectively.

IV. CONDUCTIVE LAYER INSIDE A MEDIUM WITH SMALLER CONDUCTIVITY

A. Current dipole source inside the layer

Consider a conductive layer, with conductivity σ (and infinite extent), that is parallel to the xz plane of the cartesian system $\mathbf{x}=(x,y,z)$. We assume that this layer has a width w, e.g., the layer extends from $y=-w/2$ to $w/2$, and that the conductivity of the surrounding medium is σ'. For comparison purposes with the results of the previous paragraph, we consider an electric current dipole source $\mathbf{I}l$ parallel to the surfaces of the layer located at the origin. The electrostatic potential inside the layer can be determined by the method of images:

$$\varphi_{2DIN}(\mathbf{x}) = l\left[\mathbf{I}\cdot\mathbf{x}/(4\pi\sigma|\mathbf{x}|^3) + \sum K^{|n|}{}_{12}\mathbf{I}\cdot\mathbf{x}_n/(4\pi\sigma|\mathbf{x}_n|^3)\right], \tag{13}$$

where the summation is performed for all positive and negative integers n; the Kelvin reflection coefficient is $K_{12}=(\sigma-\sigma')/(\sigma+\sigma')$, and $\mathbf{x}_n=\mathbf{x}+n\mathbf{w}$, where $\mathbf{w}$ is a vector of magnitude w directed along the y axis.

For the electric field inside the layer, Eq. (13) leads to:

$$\mathbf{E}_{2DIN}(\mathbf{x}) = l\left\{[3(\mathbf{I}\cdot\mathbf{x})\mathbf{x}-\mathbf{I}|\mathbf{x}|^2]/(4\pi\sigma|\mathbf{x}|^5) + \sum K^{|n|}{}_{12}[3(\mathbf{I}\cdot\mathbf{x_n})\mathbf{x_n}-\mathbf{I}|\mathbf{x_n}|^2]/(4\pi\sigma|\mathbf{x_n}|^5)\right\}. \tag{14}$$

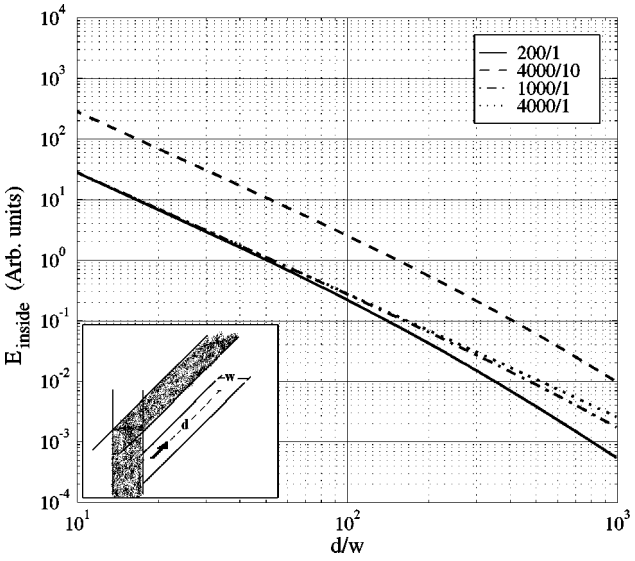

FIG. 3. The electric field E_{inside} vs the (reduced) distance d/w generated by a current dipole lying inside a conductive layer (of width w, infinite extent and conductivity σ) which is embedded in a medium (host) with conductivity σ' ($\sigma>\sigma'$). The curves correspond to the same dipole moment of the emitting source and to the conductivity ratios: $\sigma/\sigma'=4000/1$, 1000/1, 4000/10, and 200/1, respectively.

Considering, as previously, the electric field along the direction of the dipole, we plot in Fig. 3 the electric field inside the layer (labeled E_{inside}) at $y=0$ versus the distance $d=|\mathbf{x}|$ from the dipole. The ratio of this field to that for a full volume of conductivity σ' (labeled E_{host}) is shown in Fig. 4. It is smaller than unity but increases with distance, thus reflecting a decrease of E_{inside} *slower* than $1/d^3$; approximating $E_{\text{inside}}/E_{\text{host}} \propto d/w$, which holds only for a certain part (see below) of the curves depicted in Fig. 4, we find that $E_{\text{inside}} \propto 1/d^2$.

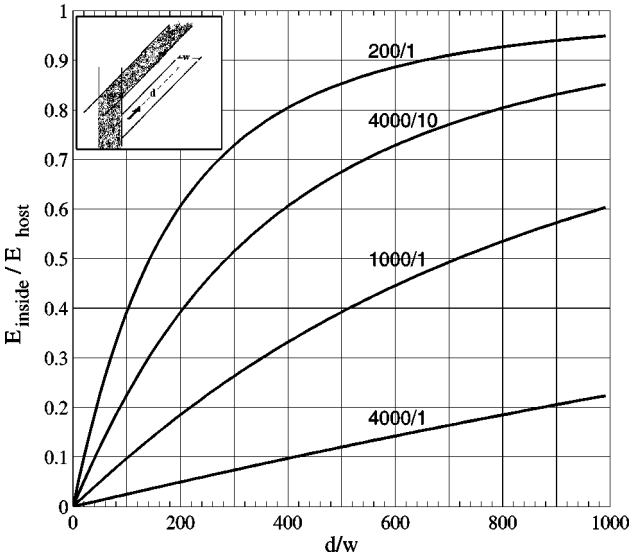

FIG. 4. The ratio $E_{\text{inside}}/E_{\text{host}}$ vs the reduced distance d/w from a current dipole lying inside a conductive layer of infinite extent (width w, conductivity σ), which is embedded in a medium (host) with conductivity σ' ($\sigma>\sigma'$). The curves correspond to the conductivity ratios: $\sigma/\sigma'=4000/1$, 1000/1, 4000/10, and 200/1, respectively.

We now proceed to a more detailed inspection of the ratio $E_{\text{inside}}/E_{\text{host}}$. It approaches σ'/σ, when d/w tends to zero, as it can be seen from the first term of the expression (14). If d/w tends to infinity, the second term is dominated by the decreasing geometrical progression {i.e., in this case the term $[3(\mathbf{I}\cdot\mathbf{x_n})\mathbf{x_n}-\mathbf{I}|\mathbf{x_n}|^2]/(4\pi\sigma|\mathbf{x_n}|^5)$ almost equals $[3(\mathbf{I}\cdot\mathbf{x})\mathbf{x}-\mathbf{I}|\mathbf{x}|^2]/(4\pi\sigma|\mathbf{x}|^5)$ for moderate values of n}; Eq. (14) then indicates that the ratio $E_{\text{inside}}/E_{\text{host}}$ tends to $(\sigma'/\sigma)[1+2K_{12}/(1-K_{12})]=1$, as expected. For a certain domain of the d/w parameter, the ratio $E_{\text{inside}}/E_{\text{host}}$ is proportional to d/w, as mentioned above. This domain can be estimated by utilizing the general expression for the potential

$$\varphi = Il\,\cos(\theta)/(4\pi\sigma d^2)\int_0^\infty \xi J_1(\xi)/R_0(\xi)\,d\xi,$$

where for points inside the layer

$$1/R_0(\xi)=\{1+(\sigma'/\sigma)\tanh[\xi w/(2d)]\}/\{(\sigma'/\sigma)+\tanh[\xi w/(2d)]\}. \tag{15}$$

For small values of $(\sigma'/\sigma)\ll 1$ and for $d>w/2$, we approximate $1/R_0(\xi)$ in the integral by $1/[(\sigma'/\sigma)+\xi w/(2d)]$; the corresponding integral is then given in closed form:[14]

$$\int_0^\infty \xi J_1(\xi)/[(\sigma'/\sigma)+\xi w/(2d)]\,d\xi = 2\pi(d/w)^2(\sigma'/\sigma)\{N_{-1}[(2d\sigma')/(w\sigma)] - \mathbf{H}_{-1}[(2d\sigma')/(w\sigma)]\}, \tag{16}$$

where $\mathbf{H}_{-1}$, N_{-1} are the Struve and Neumann functions of order -1. From Eqs. (15) and (16), and the asymptotic expression for the Struve and Neumann function (at small values of their arguments), we find that the deviation of the ratio $E_{\text{inside}}/E_{\text{host}}$ from the linear dependence is *significant* only for values of $d/w>(1/e)(\sigma/\sigma')$. Obviously, in the case $\sigma'=0$, this linear behavior holds for arbitrarily large values of d/R, resulting to a $1/d^2$ behavior for the electric field inside the layer.

In summary, we can state that, for very large conductivity ratios, i.e., $\sigma/\sigma'\gg 1$, the electric field inside the layer varies as $1/d^2$, for distances larger than the width of the layer but smaller than $(1/e)(\sigma/\sigma')w$.

When comparing Figs. 2 and 4 we conclude, as expected, that the electric field E_{2D} inside a conductive layer is smaller than E_{1D} inside a conductive cylinder (see Fig. 5). For a given conductivity ratio, the ratio E_{1D}/E_{2D} reaches a maximum, at a certain distance, but it approaches unity at appreciably larger distances.

V. CURRENT DIPOLE SOURCE OUTSIDE A CONDUCTIVE PATH

We explain below how the previous calculations, described in Secs. III and IV, are carried out when the (point) dipole emitting source lies at a distance D from the conductive path.

We start with a *conductive cylinder* of infinite length. The dipole current source $\mathbf{I}l$ is located at the point $(\rho_0,\varphi_0,Z_0)=(D,0,0)$, of the cylindrical coordinate system,

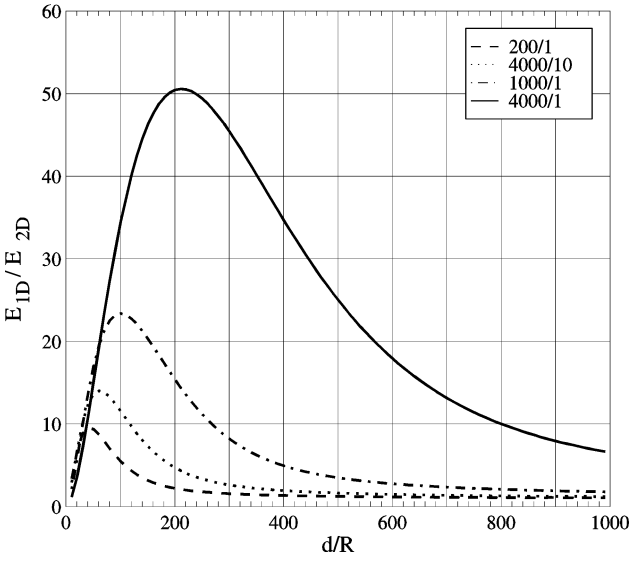

FIG. 5. The ratio E_{1D}/E_{2D} (i.e., the ratio of the electric field inside a conductive cylinder, of infinite length and radius R, to the electric field inside a conductive layer of width $w=R$ and infinite extent) vs the reduced distance d/R from a current dipole. The curves correspond to the conductivity ratios: $\sigma/\sigma'=4000/1$, 1000/1, 4000/10, and 200/1, respectively.

outside the cylinder $(D>R)$ and parallel to its axis. In this case, the expression that was used for the expansion of the Green's function into modified Bessel functions, should be replaced by the following more general expression, which holds for $\rho<\rho_0$ (see Ref. 14, Eq. 8.530.2, p. 979 and Eq. 6.671.14, p. 732)

$$\varphi^p = I/\{4\pi\sigma'[\rho^2+\rho_0^2-2\rho\rho_0\,\cos(\varphi)+z^2]^{1/2}\} = I/(2\pi^2\sigma' R)\sum\,\epsilon_m\,\cos(m\varphi) \times\int_0^\infty I_m(\xi\rho/R)K_m(\xi\rho_0/R)\cos(\xi z/R)\,d\xi,$$

where the summation is over all non-negative integers and $\epsilon_0=1$ and $\epsilon_m=2$, otherwise. For the secondary fields, we use, as in Sec. III, combinations of I_m and K_m for points inside and outside the cylinder, respectively. Utilizing the above expression and the boundary conditions, i.e., Eqs. (3) and (4), we obtain:

$$\varphi_{\text{IN}} = Il/(2\pi^2\sigma' R^2)\sum\,\epsilon_m\,\cos(m\varphi) \times\int_0^\infty \xi I_m(\xi\rho/R)A_m(\xi)\sin(\xi z/R)\,d\xi,$$

and

$$\varphi_{\text{OUT}} = Il/(2\pi^2\sigma' R^2)\Big(zR^2/[\rho^2+D^2-2\rho D\,\cos(\varphi)+z^2]^{3/2}+\sum\,\epsilon_m\,\cos(m\varphi)\int_0^\infty \xi K_m(\xi\rho/R) \times B_m(\xi)\sin(\xi z/R)\,d\xi\Big),$$

where

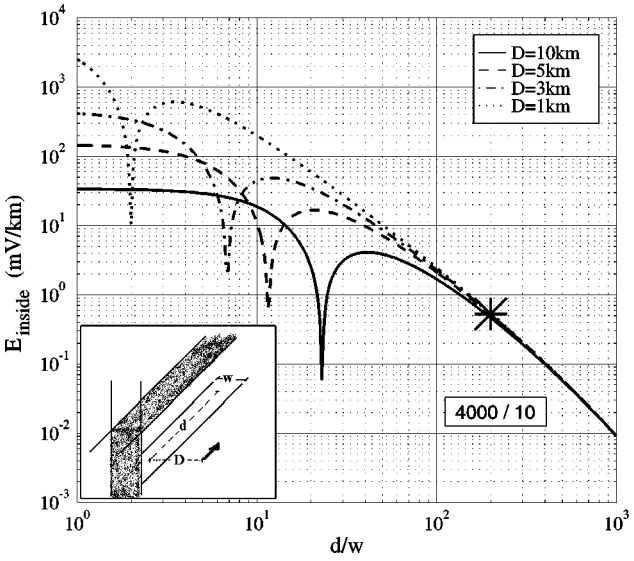

FIG. 6. The absolute value of E_{inside} vs d/w, for various values of the distance D (=1,3,5,10 km, see the inset) of the emitting dipole from a given conductive layer ($w=500$ m). Note that, for values $d/w \approx 10^2$ or larger, all curves practically coincide. Conductivity ratio $\sigma/\sigma' = 4000/10$. The ''anomaly,'' i.e., the abrupt decrease and then increase of E_{inside} at certain values of d/w, simply reflects the fact that E_{inside} changes sign (passing through zero), while the absolute value of the (total) electric field remains finite (due to the existence of the perpendicular component).

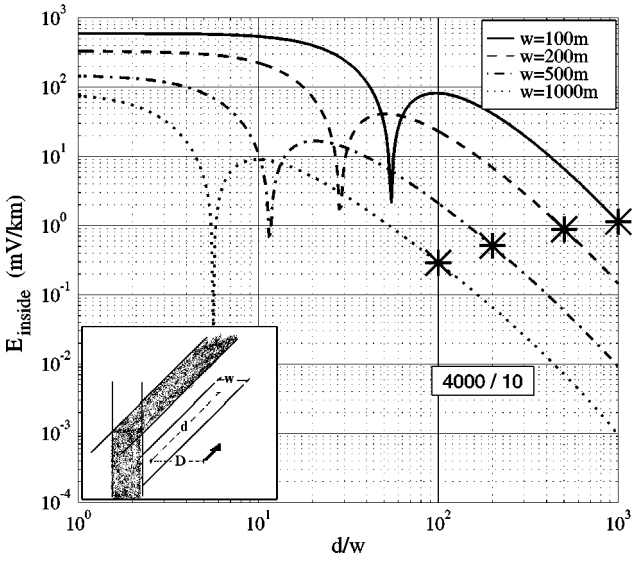

FIG. 7. The absolute value of E_{inside} vs d/w, for various values of the width w (=100,200,500,1000 m, see the inset) of the layer, but for the same D value, i.e., $D=5$ km. The points with asterisks correspond to $d \approx 100$ km. Conductivity ratio $\sigma/\sigma' = 4000/10$.

$$A_m(\xi) = (1/\xi)K_m(\xi D/R)/[I_m(\xi)K'_m(\xi) - (\sigma/\sigma')I'_m(\xi)K_m(\xi)]$$

and

$$B_m(\xi) = [I_m(\xi)/K_m(\xi)][A_m(\xi) - K_m(\xi D/R)].$$

We now turn to a *conductive layer* of infinite extent. The dipole current source $\mathbf{I}l$ is parallel to the z axis and is located at the point $(x_0, y_0, z_0) = (0, D, 0)$ of the Cartesian system. The potential at the $(x,0,z)$ plane can be easily found by using the method of images

$$\varphi(x,0,z) = Il/[4\pi(\sigma+\sigma')]\left\{ z/(x^2+z^2+D^2)^{3/2} + 2\sum [(\sigma-\sigma')/(\sigma+\sigma')]^n z/ [x^2+z^2+(D+nw)^2]^{3/2} \right\},$$

where the summation is over all positive integers.

Examples of the aforementioned calculations are depicted in Figs. 6–9, which will be discussed in the next section.

VI. DISCUSSION

Figures 2 and 4 show that, for large conductivity ratios, e.g., $\sigma/\sigma' \approx 1000/1$ to 4000/10, and for distances of practical interest, i.e., d/R (or d/w) ≈ 1 to 10^3, when measuring the electric field inside the conductive path (cylinder or layer), the following general behavior is observed:

(a) at relatively small (reduced) distances from the emitting source, E_{inside} is drastically smaller than the field E_{host}, which would be measured if the conductive path were not present;

(b) at large (reduced) distances, i.e., d/R (or d/w) $\approx a$ few hundreds to several hundreds, E_{inside} becomes comparable (within a small factor of around 3, or so) with the value of E_{host}. This behavior is a result of the fact that E_{inside} decreases with distance at a slower rate than E_{host}.

(c) We emphasize that the above result, i.e., at large distances $E_{\text{inside}} \approx E_{\text{host}}$, should not be misinterpreted as

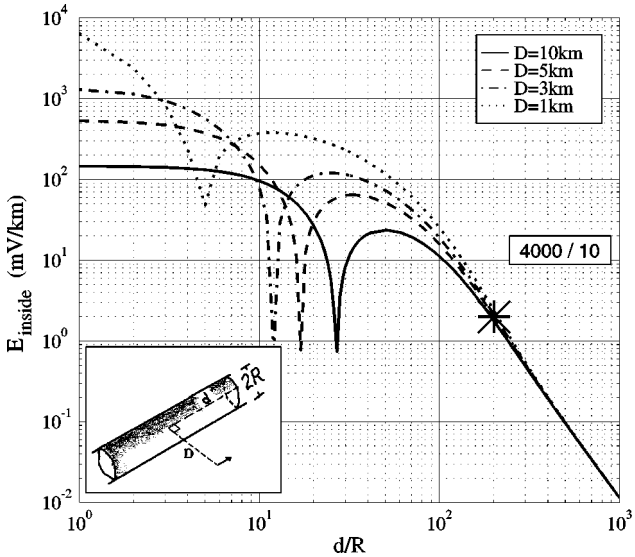

FIG. 8. The absolute value of E_{inside} vs d/R, for various values of the distance D (=1,3,5,10 km, see the inset) of the emitting dipole from a given conductive cylinder ($R=500$ m). Note that, for values $d/R \approx 2\times 10^2$ or larger, all curves practically coincide. Conductivity ratio $\sigma/\sigma' = 4000/10$.

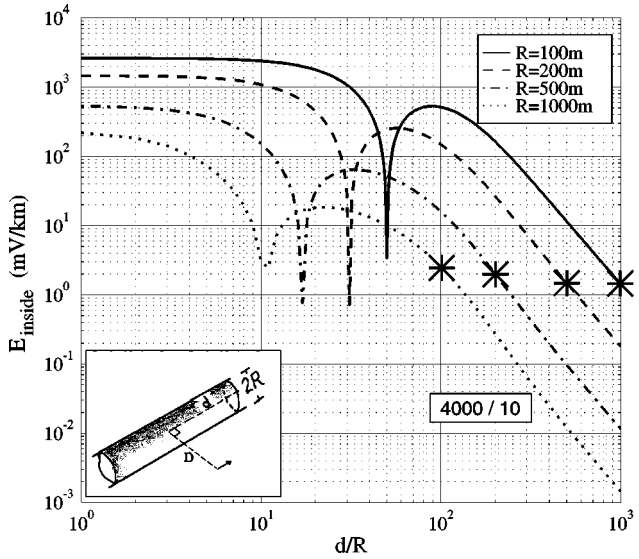

FIG. 9. The absolute value of E_{inside} vs d/R, for various values of the radius R (=100,200,500,1000 m, see the inset) of the conductive cylinder, but for the same D value, i.e., $D=5$ km. The points with asterisks correspond to $d\approx 100$ km. Conductivity ratio $\sigma/\sigma'=4000/10$.

indicating that the presence of the conductive path has no practical influence on the electric field measurements. This will be explained below.

(d) The current density j (along the direction of the emitting dipole), inside and *just* outside the conductive path, is given by $j_{\text{inside}}=\sigma E_{\text{inside}}$ and $j_{\text{outside}}=\sigma' E_{\text{outside}}$, and hence $j_{\text{inside}}/j_{\text{outside}}=\sigma/\sigma'$. At large distances, as explained above, $E_{\text{outside}}\approx E_{\text{host}}$ and $E_{\text{inside}}\approx E_{\text{host}}$; the last two relations hold at any remote site $d=d_2$, if the conductive path has an infinite length. If we assume that the conductive path terminates at $d=d_2$, we then expect a current density to have an absolute value smaller than, but of the order of $|j_{\text{inside}}|$, at some points ($d\lesssim d_2$) outside the highly conductive path, but close to the outcrop (*edge effect*). Therefore, at these points, the electric field $|E_{\text{outside}}|$ should be of the order of $|j_{\text{inside}}|/\sigma'$ and hence:

$$|E_{\text{outside}}|\approx|j_{\text{inside}}|/\sigma'\approx|E_{\text{host}}|(\sigma/\sigma').$$

The last relation reveals that, at some points of the host medium close to the termination of the conductive path, the value of the electric field exceeds $|E_{\text{host}}|$ by a factor which is of the order of the conductivity ratio σ/σ' (cf. a quantitative argument, for a simple geometry, is given in the appendix). As the latter may be as high as $\sim 10^3$, this implies the following interesting phenomenon: the electric field value may decrease by a significant factor, e.g., $\sim 10^3$ (at d_2 due to the increased separation from the source), and then it may be enhanced (at some points $d\lesssim d_2$ within the host medium) by a comparable factor, i.e., $\sim 10^3$ because of the large value σ/σ'; for example, consider $\sigma/\sigma'=1000/1$, and compare the points $d_1/R\approx 10$ or $d_1/w\approx 10$ with $d_2/R\approx 500$ or $d_2/w\approx 500$ in Figs. 1 and 3, respectively. Thus, in such a case, we may measure values of the electric field, at remote sites, that are comparable to (or smaller by a factor of around 10 than) the E values close to the source. We draw attention to the point that, in the latter example, a simplified calculation based on a $1/d^3$ behavior would have led to a drastic decrease of the field, i.e., by a factor of $(500/10)^3\approx 10^5$, and hence it might have resulted in the wrong conclusion that E is not detectable at the remote site.

Large conductivity contrasts (e.g., $4\times 10^2-10^3$, or so) are usual in the case of the earth. Hence, similar implications should hold for the very low frequency transient electric signals, less than 0.1 Hz (i.e., the so called seismic electric signals, SES) that are measured[5] prior to earthquakes (EQ). The SES amplitude, at epicentral distances of the order of 100 km, is of the order of 10^{-5} V/m, well above typical noise levels, which are usually below 10^{-6} V/m. According to well accepted concepts, EQs occur by slip on faults which may have lengths of several tens of kilometers and widths of several hundred meters. The resistivities of faults have been found to be around a few Ω m–10 Ω m, thus being 10^2-10^3 times more conductive than the surrounding medium, which, at a usual depth of 5–30 km, has a resistivity of 10^3 to 10^4 Ω m. Thus, in the case of SES the emitting source (i.e., the EQ preparation zone, where stresses are ''accumulating'' before rupture) *should* lie at a small distance D from a neighboring conductive path. We shall show below that, if the electric field measurements are carried out at a remote site, i.e., $d\gg D$, the conclusions (as far as the SES detectability is concerned) do not depend on the exact values that were selected either for the distance D or for the width of the path.

We first inspect the values involved in such a calculation, which is carried out in a way described in Sec. V: let us assume that the distance D may have any value in the range 1–10 km, and the width w in the range 100–1000 m (cf. in the literature, a fault is usually assumed to have a width of around 500 m). For simplicity, the emitting source is assumed as a point dipole parallel to the axis of the cylinder or to the layer, respectively. The dipole moment, as mentioned in Sec. II, was estimated by Slifkin[9] to be 8×10^{-4} C m, after considering a slab with a length of $L\approx 1$ km and a cross-sectional area of 1000 m$\times$100 m$=0.1$ km^2. Considering a typical seismic source of (magnitude) $M\approx 5$, it has a length of around 5 km and a cross-sectional area of around 1 km^2; comparable values may be assumed for the emitting electric source, although the stressed volume may have larger dimensions than those of the seismic source. Therefore, even if we assume a modest value for the density of dislocations, i.e., $4\times 10^7/\text{m}^2$—see Sec. II—(and disregarding—for the purpose of our calculation—factors of around 2 or so) we may estimate that the relevant emitting source should have a dipole moment larger than that estimated by Slifkin[9] by a factor of the order of 10^2; this value will be used below, although we could have accepted even a larger density of dislocations.

Figures 6 and 7 depict, for a conductivity ratio $\sigma/\sigma'=4000/10$, the electric field E_{inside} vs d/w for various values of the parameters D and w, respectively. Similarly, Figs. 8 and 9 depict, for a conductive cylinder, E_{inside} vs d/R for various values of D and R, respectively. An inspection of these figures indicates the following: although the curves of

Fig. 6 have been plotted for different D values (cf. but for a given layer, i.e., $w=500$ m), their electric field values all coincide at large distances; the same holds for the curves of Fig. 8, which correspond to various D values from a given cylinder, i.e., $R=500$ m. This behavior is consistent with the conclusions of Sec. III and IV, according to which E_{inside} should approach E_{host} at large values of d/w or d/R, respectively. For example, in the case of a conductive layer, at $d/w\approx 200$ (which corresponds to $d\approx 100$ km), Fig. 6 shows that $E_{\text{inside}}\approx 0.5$ mV/km; this value is not seriously affected if we change the width w from 100 to 1000 m (compare the points with the asterisks in Fig. 7). A similar example can be considered for a conductive cylinder: Fig. 8 shows, at $d/R\approx 200$ (which corresponds to $d\approx 100$ km for $R\approx 500$ m), $E_{\text{inside}}\approx 2$ mV/km; this E_{inside} value is not seriously affected, as shown by the asterisks in Fig. 9 if we change R in the range 100–1000 m. The results of these two examples are consistent with the contents of Secs. III and IV, if we inspect Figs. 2 and 4 for $d/R\approx 200$ and $d/w\approx 200$, respectively: For $\sigma/\sigma'=4000/10$, they show $E_{\text{inside}}/E_{\text{host}}\approx 1.7$ and $E_{\text{inside}}/E_{\text{host}}\approx 0.4$, respectively (cf. the value of E_{inside} in the conductive cylinder exceeds that inside the conductive layer by a factor of around 4, as indicated in Fig. 5). Disregarding such small factors, the main point is that for large distances of practical interest, e.g., $d/R\approx 200$ or $d/w\approx 200$, E_{inside} is comparable with E_{host}. As the above calculation was carried out for a layer of infinite extent, or for a conductive cylinder of infinite length, respectively, we expect that the estimated electric field value of the order of 1 mV/km should be enchanced, as mentioned above, by a factor almost equal to the conductivity ratio when measuring it in the host medium but in the vicinity of the outcrop (''*edge effects*''). Therefore, the electric field becomes of the order of 10^2 mV/km, even with the modest values selected above. In summary, the order of magnitude of the electric field, in the vicinity of the outcrop of the conductive path, is not affected by any specific selection of the values of w (or R) and D, as long as $d\gg w$ (or R), D. (cf. a numerical solution of Maxwell equations[15] indicates that the value of w or R, respectively, regulates the extent of the region in which the electric field is measurable on the earth's surface). We clarify that the measured value, at large distances, is controlled by the following *three* parameters, whose (lowest) boundaries are safely selected:

(a) *the host resistivity*, which is of the order of 10^3 Ω m,
(b) *the conductivity ratio* σ/σ', and
(c) *the moment of the emitting electric dipole*, which is primarily based on the density of charged defects.

Any increase of the values of these three quantities results in an *increase* of the electric field value estimated above. Recall that this value, of the order 10^2 mV/km, refers to sites close to the termination of the conductive path; therefore, assuming that this termination lies at small distances from the observation point on the earth's surface, it is estimated that the measured electric field value will be around 10 mV/km, which is well above typical noise levels.

The above discussion showed that, if the conductive path terminates close to the earth's surface, at $d\approx 100$ km, the electric field can reach measurable values at such remote sites, but maybe not at shorter. This behavior agrees with experimental results, i.e., the SES feature, called *selectivity effect*.[5]

The following remark should be added: Slifkin[9] also discussed the question related to the rather long duration of the recorded SES, as compared to the quite short RC time constant for relaxation of electric fields in typical wet minerals. He suggested that it is possible that the recorded SES consist of unresolved superpositions of many rapid pulses, generated by the propagation of mechanical relaxations in a sequence of neighboring blocks. This possibility will be investigated in a separate publication, along with a study of the frequency dependence of the amplitude of the signals, when they are transmitted in a medium containing high conductivity paths.

VII. CONCLUSIONS

(1) Upon *gradual* variation of pressure, a solid containing electric dipoles due to defects emits a transient (polarization or depolarization) electric signal, which reaches its maximum (absolute) value when the relation
$$\left.\frac{d\tau}{dt}\right|_{j=j_M}=-1$$
is fulfilled. This relation leads to $b\upsilon^{m,b}\tau\approx -kT$, without having to assume that the pressure rate remains constant.
(2) The variation of the electric field E_{inside} versus the distance d from an emitting dipole source was studied, when the signal is transmitted through a high conductivity path embedded in a less conductive medium. As examples of such a path, we considered two ideal cases: a cylindrical channel of infinite length, and a conductive layer of infinite extent. For large conductivity ratios σ/σ' and for distances of practical interest, the main conclusions are:
   (a) The electric field E_{inside}, inside a cylindrical channel, varies as $1/d$, compared to an $1/d^3$ behavior in an isotropic and homogeneous medium; this holds almost up to a certain (reduced) distance $(d/R)_{\text{infl}}$, which increases with the conductivity ratio σ/σ'.
   (b) The electric field, inside the layer, varies as $1/d^2$; this holds up to a certain (reduced) distance (d/w), which is around $(1/e)(\sigma/\sigma')$.
   (c) In both conductive paths (cylinder, layer), and at distances appreciably larger than those mentioned above in (a) and (b), the electric field E_{inside} becomes comparable to E_{host}, i.e., to the value that would be measured for a full volume of conductivity σ'. This implies a high value of the current density inside the path, because $j_{\text{inside}}/j_{\text{host}}\approx\sigma/\sigma'$.
(3) When the conductive path terminates within the host medium, ''edge effects'' play a prominent role in the electric field values measured (at the host medium but) close to the outcrop.
(4) If the aforementioned concepts in (2) and (3) are disregarded, the calculations at large distances lead to E values that underestimate their actual values by many orders of magnitude.

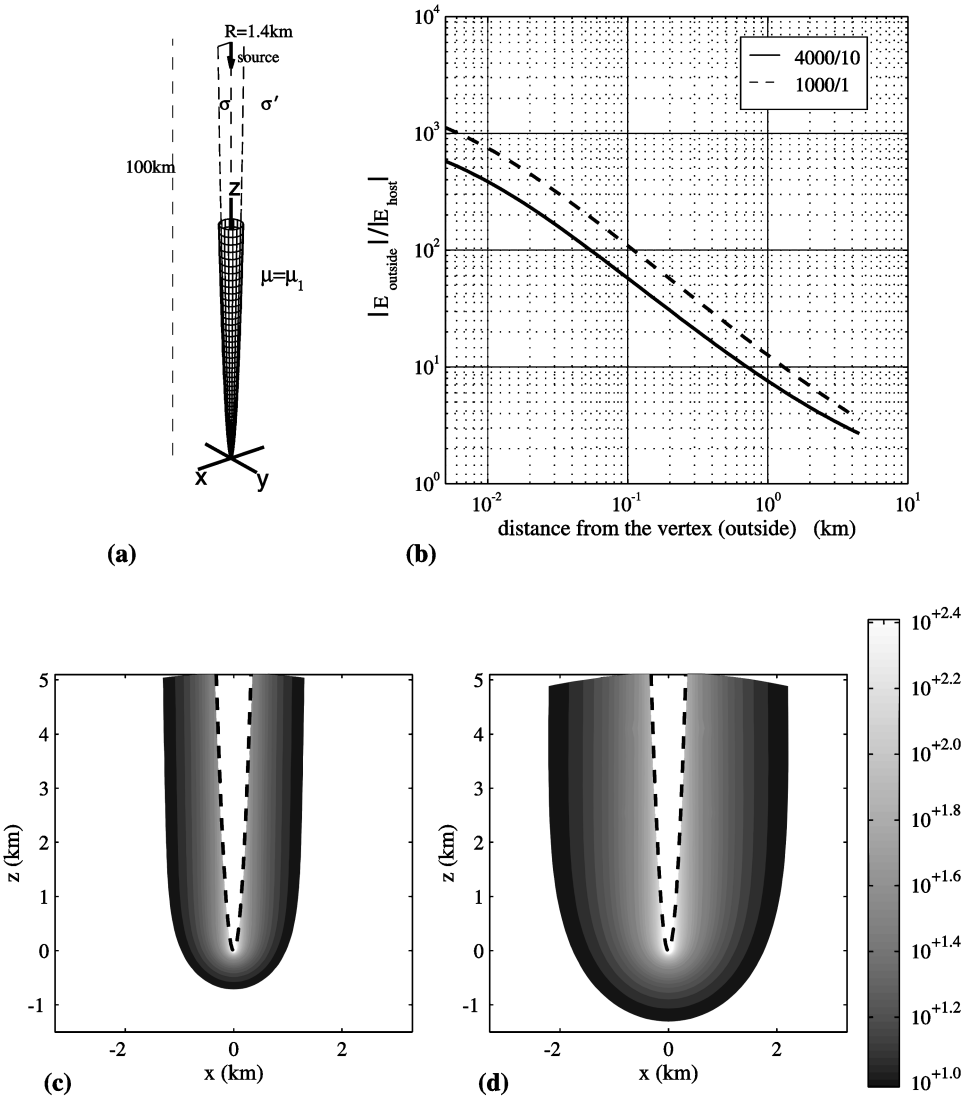

FIG. 10. Calculation of the enhancement of the electric field in the case of a paraboloidal edge for two conductivity ratios, i.e., $\sigma/\sigma' = 4000/10$, 1000/1 (a) schematic diagram of the surface, $\mu = \mu_1$, separating the regions with conductivities σ and σ' for $\mu_1 = 0.1\ \sqrt{\text{km}}$; (b) the ratio $|E_{\text{outside}}|/|E_{\text{host}}|$ along the z axis vs the distance from the vertex; (c), (d) the contours of the ratio $|E_{\text{outside}}|/|E_{\text{host}}|$ for $\sigma/\sigma' = 4000/10$ and 1000/1, respectively (the broken line depicts the surface $\mu = \mu_1$).

(5) As an application, we considered the case of the transmission of very low frequency electric signals in the der of 10 mV/km, at distances of the order of $d \approx 100$ km, but close to the outcrop of the conductive path. This conclusion does not depend on the exact values we may select, either for the distance of the emitting dipole from the neighboring highly conductive path, or for the width of this path. The electric field values estimated in this article coincide with those independently obtained by numerical solutions of Maxwell equations.[15] The present results are in basic agreement with the suggestion of Lazarus,[10] who stated that these signals ''would be channeled into strata...and would propagate through these paths...quite analogous to...electrical signals through wires.''

ACKNOWLEDGMENTS

We would like to express our sincere thanks to Professor S. Uyeda, Professor D. Lazarus, Professor K. Alexopoulos, Professor F. Hadjioannou, Professor A. Lahanas, and Professor P. Ioannou for very useful discussions. We would like to dedicate this paper to Professor David Lazarus on the occasion of his 75th birthday.

APPENDIX A: ELECTRIC FIELD CALCULATION IN THE CASE OF A PARABOLOIDAL ''EDGE''

Consider a paraboloidal region of conductivity σ embedded in a host medium of conductivity σ'. We assume that $\sigma \gg \sigma'$ and make use of the paraboloidal coordinates[16]

$$x = \lambda\mu\ \cos(\varphi), y = \lambda\mu\ \sin(\varphi), z = 1/2(\lambda^2 - \mu^2),$$

where $\varphi \in [0, 2\pi]$, $\mu, \lambda \in [0, \infty]$. The surfaces of equal λ and μ are parabolic surfaces of revolution, and the equal φ surfaces are planes that intersect each other along the z axis. The Laplacian in the paraboloidal coordinates is given by

$$\nabla^2\psi = 1/[\lambda\mu(\lambda^2 + \mu^2)][\mu\partial/\partial\lambda(\lambda\partial\psi/\partial\lambda)$$

$$+\lambda\partial/\partial\mu(\mu\partial\psi/\partial\mu)+(\lambda^2+\mu^2)/(\lambda\mu)\partial^2\psi/\partial\varphi^2]. \tag{A1}$$

We suppose that the conductivity in the region $\mu<\mu_1$ bounded by the paraboloid $\mu=\mu_1$ is σ, and for the space outside $\mu\geqslant\mu_1$ is σ'. We study the case of a point current source I located at the z axis $(0,0,z_0)$ with paraboloidal coordinates $(\mu_0=0,\lambda_0=\sqrt{2z_0},\varphi_0=0)$. In view of the azimuthal symmetry, the solution of the Laplace [Eq. (A1)] can be separated as $A(k)J_0(k\lambda)I_0(k\mu)$ for $\mu<\mu_1$, and $B(k)J_0(k\lambda)K_0(k\mu)$ for $\mu\geqslant\mu_1$. The singular primary potential (inside the paraboloidal insert) due to the point current source is given by[16]

$$\varphi^p=I/(2\pi\sigma)\int_0^\infty J_0(k\lambda)J_0(k\lambda_0)K_0(k\mu)kdk. \tag{A2}$$

Adding to this primary potential, the two separated forms of the solution of the Laplace equation, we obtain

$$\varphi_{\mathrm{IN}}=I/(2\pi\sigma)\int_0^\infty J_0(k\lambda)J_0(k\lambda_0)K_0(k\mu)kdk + \int_0^\infty A(k)J_0(k\lambda)J_0(k\lambda_0)I_0(k\mu)kdk, \tag{A3}$$

$$\varphi_{\mathrm{OUT}}=\int_0^\infty B(k)J_0(k\lambda)J_0(k\lambda_0)K_0(k\mu)kdk, \tag{A4}$$

where

$$A(k)=I/(2\pi)(1-\sigma'/\sigma)K_0(k\mu_1)K_1(k\mu_1)/[\sigma'K_1(k\mu_1)I_0(k\mu_1)+\sigma K_0(k\mu_1)I_1(k\mu_1)], \tag{A5}$$

and

$$B(k)=I/\{(2\pi k\mu_1)[\sigma'K_1(k\mu_1)I_0(k\mu_1)+\sigma K_0(k\mu_1)I_1(k\mu_1)]\}, \tag{A6}$$

which have been found by applying the appropriate boundary conditions:

$$E_{\lambda\mathrm{IN}}=E_{\lambda\mathrm{OUT}} \quad \text{and} \quad \sigma E_{\mu\mathrm{IN}}=\sigma' E_{\mu\mathrm{OUT}} \tag{A7}$$

at the surface $\mu=\mu_1$.

Equations (A3) and (A4) allow the calculation of the potential at any point; by combining a source I at a point z_0 and a sink $-I$ at z_0-l, we obtain the potential due to a current electric dipole source. As an example, such a calculation has been made for two conductivity ratios, i.e., $\sigma/\sigma'=4000/10$, $1000/1$, and for the case $\mu_1=0.1\sqrt{\mathrm{km}}$, by considering a dipole source (lying inside the conductive medium) at a distance of $z_0=100$ km from the vertex of the paraboloid. The main results are depicted in Fig. 10, which shows that (for both conductivity ratios) near the vertex $|E_{\mathrm{outside}}|/|E_{\mathrm{host}}|\approx\sigma/\sigma'$, as mentioned in the main text. Furthermore, note that the contours depicted in Fig. 10(c) and 10(d) indicate that there is a considerable area, ''surrounding the edge,'' in which $|E_{\mathrm{outside}}|$ exceeds $|E_{\mathrm{host}}|$ by a significant factor, e.g., 10 or larger.

[1] P. Varotsos and K. Alexopoulos, in *Thermodynamics of Point Defects and their Relation with Bulk Properties*, edited by S. Amelinckx, R. Gevers, and J. Nihoul (North Holland, Amsterdam, 1986).
[2] D. N. Yoon and D. Lazarus, Phys. Rev. B **5**, 4935 (1972); P. C. Allen and D. Lazarus, *ibid.* **17**, 1913 (1978); A. E. Pontau and D. Lazarus, *ibid.* **19**, 4027 (1979); J. Oberschmidt and D. Lazarus, *ibid.* **21**, 2952 (1980); *ibid.* **21**, 5813 (1980); B. E. Mellander and D. Lazarus, *ibid.* **29**, 2148 (1984).
[3] P. Varotsos and K. Alexopoulos, Phys. Rev. B **21**, 4898 (1980).
[4] J. J. Fontanella, C. A. Edmondson, and M. C. Wintersgill, Macromolecules **29**, 4944 (1996).
[5] P. Varotsos, K. Alexopoulos, K. Nomicos, and M. Lazaridou, Nature (London) **322**, 120 (1986); P. Varotsos and M. Lazaridou, Tectonophysics **188**, 321 (1991); P. Varotsos, K. Alexopoulos, and M. Lazaridou, *ibid.* **224**, 1 (1993).
[6] L. M. Slifkin, in *Diffusion in Materials*, edited by A. L. Laskar, J. L. Bocquet, G. Brebec, and C. Monty (Kluwer, Dordrecht, 1990), Vol. 179, p. 471.
[7] P. Varotsos, N. Bogris, and A. Kiritsis, J. Phys. Chem. Solids **53**, 1007 (1992), in this paper only the case of PSDC was discussed.
[8] P. Varotsos, Phys. Status Solidi B **90**, 339 (1978); J. Appl. Phys. **51**, 4553 (1980).
[9] L. M. Slifkin, in *The Critical Review of VAN: Earthquake Prediction from Seismic Electric Signals*, edited by Sir J. Lighthill (World Scientific, Singapore, 1996), p. 97; Tectonophysics **224**, 149 (1993).
[10] D. Lazarus, in *The Critical Review of VAN: Earthquake Prediction from Seismic Electric Signals*, edited by Sir J. Lighthill (World Scientific, Singapore, 1996), p. 91; Tectonophysics **224**, 265 (1993).
[11] M. Abramowitz and I. Stegun, *Handbook of Mathematical Functions* (Dover, New York, 1970).
[12] J. R. Wait, Colorado School Mines Q. **73**, 1 (1978).
[13] A. H. Zemanian, in *Distribution Theory and Transform Analysis* (Dover, New York, 1987), p. 180.
[14] I. S. Gradshteyn and I. M. Ryzhik, in *Table of Integrals, Series and Products* (Academic, San Diego, 1980), Equation 6.562.2, p. 685.
[15] P. Varotsos, N. Sarlis, M. Lazaridou, and P. Kapiris, Practica of the Athens Academy **71**, 283 (1996); *ibid.* (in press).
[16] P. Morse and H. Feshbach, in *Methods of Theoretical Physics* (McGraw-Hill, New York, 1954), pp. 1296–1298.